A Vortex Relocation Scheme for Tropical Cyclone Initialization in Advanced Research WRF

LING-FENG HSIAO

Central Weather Bureau, and Taiwan Typhoon and Flood Research Institute, Taipei, Taiwan

CHI-SANN LIOU

Naval Research Laboratory, Monterey, California

TIEN-CHIANG YEH

Central Weather Bureau, Taipei, Taiwan

YONG-RUN GUO

National Center for Atmospheric Research, Boulder, Colorado

DER-SONG CHEN, KANG-NING HUANG, CHUEN-TEYR TERNG, AND JEN-HER CHEN

Central Weather Bureau, Taipei, Taiwan

(Manuscript received 6 November 2009, in final form 23 February 2010)

ABSTRACT

This paper introduces a relocation scheme for tropical cyclone (TC) initialization in the Advanced Research Weather Research and Forecasting (ARW-WRF) model and demonstrates its application to 70 forecasts of Typhoons Sinlaku (2008), Jangmi (2008), and Linfa (2009) for which Taiwan's Central Weather Bureau (CWB) issued typhoon warnings. An efficient and dynamically consistent TC vortex relocation scheme for the WRF terrain-following mass coordinate has been developed to improve the first guess of the TC analysis, and hence improves the tropical cyclone initialization. The vortex relocation scheme separates the first-guess atmospheric flow into a TC circulation and environmental flow, relocates the TC circulation to its observed location, and adds the relocated TC circulation back to the environmental flow to obtain the updated first guess with a correct TC position. Analysis of these typhoon cases indicates that the relocation procedure moves the typhoon circulation to the observed typhoon position without generating discontinuities or sharp gradients in the first guess.

Numerical experiments with and without the vortex relocation procedure for Typhoons Sinlaku, Jangmi, and Linfa forecasts show that about 67% of the first-guess fields need a vortex relocation to correct typhoon position errors while eliminates the topographical effect. As the vortex relocation effectively removes the typhoon position errors in the analysis, the simulated typhoon tracks are considerably improved for all forecast times, especially in the early periods as large adjustments appeared without the vortex relocation. Comparison of the horizontal and vertical vortex structures shows that large errors in the first-guess fields due to an incorrect typhoon position are eliminated by the vortex relocation scheme and that the analyzed typhoon circulation is stronger and more symmetric without distortions, and better agrees with observations. The result suggests that the main difficulty of objective analysis methods [e.g., three-dimensional variational data assimilation (3DVAR)], in TC analysis comes from poor first-guess fields with incorrect TC positions rather than not enough model resolution or observations. In addition, by computing the eccentricity and correlation of the axes of the initial typhoon circulation, the distorted typhoon circulation caused by the position error without the vortex relocation scheme is demonstrated to be responsible for larger track errors. Therefore, by eliminating the typhoon position error in the first guess that avoids a distorted initial typhoon circulation, the vortex relocation scheme is able to improve the ARW-WRF typhoon initialization and forecasts particularly when using data assimilation update cycling.

Corresponding author address: Ling-Feng Hsiao, Central Weather Bureau, No. 64, Gongyuan Road, 10048 Taipei, Taiwan.
E-mail: lfhsiao@rdc.cwb.gov.tw

DOI: 10.1175/2010MWR3275.1

Report Documentation Page

Form Approved
OMB No. 0704-0188

1. REPORT DATE	2. REPORT TYPE	3. DATES COVERED
2010		**00-00-2010 to 00-00-2010**

4. TITLE AND SUBTITLE	5a. CONTRACT NUMBER
A Vortex Relocation Scheme for Tropical Cyclone Initialization in Advanced Research WRF	5b. GRANT NUMBER
	5c. PROGRAM ELEMENT NUMBER
6. AUTHOR(S)	5d. PROJECT NUMBER
	5e. TASK NUMBER
	5f. WORK UNIT NUMBER
7. PERFORMING ORGANIZATION NAME(S) AND ADDRESS(ES) **Central Weather Bureau, and Taiwan and Flood Research Institute,,Taipei, Taiwan, , ,**	8. PERFORMING ORGANIZATION REPORT NUMBER
9. SPONSORING/MONITORING AGENCY NAME(S) AND ADDRESS(ES)	10. SPONSOR/MONITOR'S ACRONYM(S)
	11. SPONSOR/MONITOR'S REPORT NUMBER(S)

12. DISTRIBUTION/AVAILABILITY STATEMENT
Approved for public release; distribution unlimited

13. SUPPLEMENTARY NOTES
This study was financially supported by the National Science Council of the R.O.C. under Grants NSC96-2625-Z-052-003 and NSC97-2625-M-052-002; and (for the second author) by the Office of Naval Research through Program PE-0602435N.

14. ABSTRACT
This paper introduces a relocation scheme for tropical cyclone (TC) initialization in the Advanced Research Weather Research and Forecasting (ARW-WRF) model and demonstrates its application to 70 forecasts of Typhoons Sinlaku (2008), Jangmi (2008), and Linfa (2009) for which Taiwan?s Central Weather Bureau (CWB) issued typhoon warnings. An efficient and dynamically consistent TC vortex relocation scheme for the WRF terrain-following mass coordinate has been developed to improve the first guess of the TC analysis, and hence improves the tropical cyclone initialization. The vortex relocation scheme separates the first-guess atmospheric flow into a TC circulation and environmental flow, relocates the TC circulation to its observed location, and adds the relocated TC circulation back to the environmental flow to obtain the updated first guess with a correct TC position. Analysis of these typhoon cases indicates that the relocation procedure moves the typhoon circulation to the observed typhoon position without generating discontinuities or sharp gradients in the first guess.

15. SUBJECT TERMS

16. SECURITY CLASSIFICATION OF:			17. LIMITATION OF ABSTRACT	18. NUMBER OF PAGES	19a. NAME OF RESPONSIBLE PERSON
a. REPORT	b. ABSTRACT	c. THIS PAGE			
unclassified	**unclassified**	**unclassified**	**Public Release**	**18**	

1. Introduction

The community Weather Research and Forecasting (WRF) modeling system is a mesoscale forecast and data assimilation system that is designed to advance both atmospheric research and operational prediction (Skamarock et al. 2008). It has been used for atmospheric research including the study of mesoscale convective systems, tropical cyclones (TCs), and large eddy studies (e.g., Jankov et al. 2005; Davis et al. 2008; Moeng et al. 2007). The WRF has also been used by several numerical weather prediction (NWP) centers in their daily operations to provide guidance for forecasters [e.g., the National Centers for Environmental Predication (NCEP), Air Force Weather Agency (AFWA), and Korea Meteorological Administration (KMA)]. At Taiwan's Central Weather Bureau (CWB), the WRF model is undergoing testing for operational use.

There are two key components for numerical TC forecasting—an accurate forecast model and a proper method to initialize tropical cyclones. Since tropical cyclones spend most of their lifetime over oceans where observational data are lacking, special effort must be taken to properly initialize numerical prediction models. The present paper proposes a method of improving TC initialization, and hence TC forecasts for the Advanced Research WRF model (ARW-WRF; Skamarock et al. 2008). In this study, we use version 3.0.1 of the ARW-WRF with a 221 $\times$ 127 grid in 45-km grid spacing to illustrate the TC initialization and forecast.

Over the last few decades, methods that supplement observations near a TC center with synthetic (or bogus) observations were developed for TC model initialization (Kurihara et al. 1990; Lord 1991; Thu and Krishnamurti 1992). However, the synthetic observational data do not include all meteorological parameters required in the assimilation analysis. As a result, the initialized TC vortex is usually out of balance with respect to the dynamics of the forecast model. To overcome the model inconsistency problem, Kurihara et al. (Kurihara et al. 1993, 1995) proposed a method of specifying an initial vortex in the Geophysical Fluid Dynamics Laboratory (GFDL) hurricane prediction model. In their work, the large-scale analysis is decomposed into environmental flow and vortex circulation. Through the time integration of an axisymmetric version of the hurricane prediction model, the symmetric vortex is generated by targeting the symmetric tangential wind component to match observed TC parameters and empirical TC structure. The asymmetric part of the initial vortex is constructed from the asymmetric perturbation of the previous 12-h forecast valid at the current time (Bender et al. 2007). The final initial condition is constructed by adding the symmetric and asymmetric parts of the initial vortex to the environmental flow.

Xiao et al. (2000) proposed the Bogus Data Assimilation (BDA) scheme to initialize tropical cyclones for numerical model forecasts. The variational initialization scheme specifies the sea level pressure of the hurricane vortex based on Fujita's formula (Fujita 1952) and then derives the wind from the gradient wind relationship. The important step is a minimization procedure that generates all other variables by integrating the forecast model. In their sensitivity study of Hurricane Fran (1996) using the BDA scheme, Xiao et al. (2000) show that the size of the specified bogus vortex has significant impacts on the simulations of the hurricane track and intensity. Meanwhile, they pointed out that, in the BDA scheme, the assimilation of sea level pressure bogus data is more effective than the wind bogus data in improving the hurricane structure. However, a different result was presented by Pu and Braun (2001) that the assimilation with the wind data is more efficient than that with the sea level pressure data. Further research by Wu et al. (2006) found that the radius of Rossby deformation was considerably different between the cases studied by Xiao et al. (2000) and Pu and Braun (2001). Therefore, the scale of the TC vortex plays a critical role on the geostrophic adjustment process in the BDA scheme.

In recent years, a vortex relocation technique was successfully developed and implemented in the Global Forecast System (GFS) at NCEP (Liu et al. 2000). The vortex relocation technique is based on the vortex separation method developed by Kurihara et al. (1995) for GFDL model TC initialization. Rather than implanting a spunup vortex, the relocation method fetches the model-predicted vortex and moves it to the observed position. The relocation method greatly reduces the false spinup problem caused by inconsistencies between the initial conditions and the model dynamics and physics. As demonstrated by Liu et al. (2006), the average of the TC track forecasts in 1999 was substantially improved not only in the GFS model, but also in the GFDL model with the improvement of 31% and 25%, respectively. In addition, the vortex relocation technique was also implemented in the Global Ensemble Forecast System (GEFS) and it significantly reduces the mean track errors of the GEFS forecast.

A similar vortex relocation method for improving TC initialization was developed and implemented in the Nonhydrostatic Forecast System (NFS) at CWB (Liou 2004). The method is also based upon the vortex separation method from Kurihara et al. (1995). In addition to the relocation technique applied for improving the

first-guess fields, the NFS optimal interpolation analysis uses 41 bogus data generated around an observed TC to help define the TC structure (Liou 2002).

There is a TC bogusing initialization method included in the preprocessing system of the WRF. The method is designed for cold start runs using background fields interpolated from global models (Davis and Low-Nam 2001). It first removes the TC circulation from the background by removing vorticity, divergence, and geostrophic vorticity within 300 km of the background TC center, and then implants an axisymmetric Rankine vortex at the observed TC location generated using observed maximum wind and a specified wind profile. The method proposed in this paper provides another typhoon initialization process in the ARW-WRF modeling system that can be integrated into the WRF data assimilation for high-resolution cycling runs.

In summary, the vortex initialization method proposed by Kurihara et al. (1993, 1995) may produce an initial vortex that is dynamically consistent with the forecast model. However, the method requires a symmetric vortex in the forecast model and the observed TC vortex structure can only be indirectly included in the initial TC vortex through nudging the wind of the spinup vortex toward the target wind derived from observed wind and an empirical wind distribution. The BDA scheme can also reduce the inconsistency between the initialized TC vortex and the model dynamics. However, it involves very costly assimilation integration and the geostrophic adjustment in the minimization procedure requires the determination of using either sea level pressure or wind bogus data depending on the scale of the TC vortex. Moreover, dynamical inconsistencies may still be generated in the forecast while the initialized TC vortex disagrees with the bogus vortex. On the other hand, the vortex relocation technique removes TC position errors, which greatly reduces the first-guess errors and eliminates double or distorted centers in the analyzed TC circulation. WRF forecasts of TC track and structure (to be shown later) indicate its tropical cyclones are not properly initialized. While considering the efficiency in initializing a TC vortex and its dynamic consistency with the forecast model, we choose the vortex relocation technique (based on the scheme implemented in the NFS) to initialize tropical cyclones in the WRF model. The main difference between the two schemes is that first-guess fields are relocated on constant pressure levels in the NFS, while first-guess fields are relocated on terrain-following sigma levels in the ARW-WRF. Section 2 describes the detailed algorithm of the vortex relocation scheme. The method is applied to TC forecasts of Typhoons Sinlaku (2008), Jangmi (2008), and Linfa (2009) for which CWB issued typhoon warnings. Sinlaku and Jangmi are two category 4 strong typhoons and Linfa is a category 1 weak typhoon. The impacts on the typhoon track and intensity forecasts are discussed in section 3. A higher-resolution nested grid of 15/5-km grid spacing is used in examining the impact on typhoon intensity forecast. Finally, conclusions are presented in section 4.

2. Methodology

The ARW-WRF model uses a terrain-following, hydrostatic-pressure vertical coordinate with the model top being a constant pressure surface. The model physics employed includes the Goddard microphysics scheme (Tao et al. 2003), the Grell–Devenyi cumulus parameterization scheme (Grell and Devenyi 2002), and the Yonsei University (YSU) planetary boundary layer scheme (Hong et al. 2006). More detailed descriptions of the WRF model can be obtained from Skamarock et al. (2008).

The procedure of the ARW-WRF version 3.0.1 consists of the following modules: (i) the WRF Preprocessing System (WPS_v3.0 plus WRF/real.exe) that generates WRF model grids including terrestrial fields and interpolates the horizontal and vertical data to the grids, (ii) the WRF three-dimensional variational data assimilation (3DVAR) that combines the observations with first-guess fields and their respective error statistics to provide an improved estimate of the atmospheric state at the analysis time, and (iii) the main module of the ARW-WRF forecast model. The vertical coordinate in the WRF model is defined as $\eta = (p_{\rm dh} - p_{\rm dht})/\mu_d$, where μ_d represents the mass of the dry air in the column and $p_{\rm dh}$ and $p_{\rm dht}$ represent the hystrostatic pressure of the dry atmosphere at the model level and model top, respectively.

The vortex relocation scheme proposed in this paper is applied after the module (i) to fix TC position errors in the first-guess fields. The modified first-guess and observational data are then assimilated by the WRF-3DVAR to get the model initial conditions. The first step of the vortex relocation scheme is to separate the TC vortex from its environmental flow in the first-guess fields. The separation procedure is similar to that described in Kurihara et al. (1995), except we use the vorticity maximum at $\eta = 0.85$ (about 850 hPa) to determine the location of the TC center for avoiding the noisy near surface, and the Barnes (1994) analysis to obtain the nonTC perturbation over the TC circulation domain. In this scheme, the computation steps are as follows:

1) To get the basic state, u_L, v_L, θ_L, γ_L, and $p_{\rm sL}$, a low-pass filter is applied to the original first-guess fields of wind (u, v), potential temperature θ, water vapor mixing ratio γ, and surface pressure p_s to filter out

disturbances with wavelengths shorter than 1200 km within a 4000 km^2 centered at the TC center. Then the perturbation fields are computed as residuals by subtracting the basic fields from the original first-guess fields.

2) To determine the range of the TC circulation, the perturbation wind at $\eta = 0.85$ is first interpolated to TC-centered polar coordinates in 24 directions. Next, azimuthally averaged tangential wind profiles are computed for the 24 directions to determine the starting radius for search. The TC edge in each direction is then determined by searching outward from the starting radius to reach a radius where the tangential wind profile satisfies one of the two conditions: $v < 6$ m s^{-1} and $\partial v/\partial r < 4 \times 10^{-6}$ s^{-1}, or $v < 3$ m s^{-1} until the search hits the outer limit set to 800 km.
3) To obtain the non-TC perturbations, $u_{\rm nt}$, $v_{\rm nt}$, $\theta_{\rm nt}$, $\gamma_{\rm nt}$, and $p_{\rm snt}$, over the TC circulation domain, a two-pass Barnes analysis (Barnes 1994) is applied using the non-TC perturbations at the TC edge as observational data. The TC vortex circulation, u_t, v_t, θ_t, γ_t, and $p_{\rm st}$, is finally computed as a residual by subtracting the non-TC perturbations from the total perturbations over the TC circulation domain.

In step 1, the 1200-km filtering wavelength is chosen as the 4 times of the 34-kt wind radius for a typical TC, which is assumed 300 km or less. The scheme is, however, not sensitive to the choice as we have compared the results from using 1200- and 1500-km filtering wavelengths and the difference is not significant (not shown). Meanwhile, instead of computing for the whole model domain, 4000 km is large enough to contain typhoon circulation before and after the relocation. In the step 2, the tangential-wind criterion used to determine the range of TC circulation is directly following the criterion used in the GFDL model (Kurihara et al. 1995). Different filtering wavelengths and tangential-wind criteria have been tested (not shown) and the results indicate that the TC relocation scheme is not sensitivity to these choices. In the step 3, the first pass of the two-pass Barnes analysis computes the non-TC perturbation at grid point g inside the TC domain as

$$x_g = \frac{\sum_{j=1,24} W_j y_j}{\sum_{k=1,24} W_k},$$

where y_j is the perturbation at the TC edge in 24 directions, $W = e^{-(r/R_1)^2}$, r is the distance between the grid point g and edge point j, and the radius of influence R_1 is set to 300 km for the first pass.

In the second pass, the non-TC perturbation at grid point g is then modified as

$$x'_g = x_g + \frac{\sum_{j=1,24} W'_j (x_j - x_a)}{\sum_{k=1,24} W'_k},$$

where x_a is the first pass result interpolated to the TC edge point j, $W' = e^{-(r/R_2)^2}$, and the radius of influence R_2 is set to 173 km. The radius of influence for each pass is chosen to provide relatively smooth but not too localized non-TC perturbation fields inside the TC domain.

The TC vortex separated by the above steps is relocated to its observed location to form the new first-guess fields in the module (i) for the WRF-3DVAR analysis. The relocated variables here are the wind (u_g, v_g), potential temperature θ_g, water vapor mixing ratio γ_g, and surface pressure $p_{\rm sg}$ computed as

$$\begin{aligned}
u_g &= u - u_t + u_t(\text{new TC location}) = u + \tilde{u},\\
v_g &= v - v_t + v_t(\text{new TC location}) = v + \tilde{v},\\
\theta_g &= \theta - \theta_t + \theta_t(\text{new TC location}) = \theta + \tilde{\theta},\\
\gamma_g &= \gamma - \gamma_t + \gamma_t(\text{new TC location}) = \gamma + \tilde{\gamma},\\
p_{\rm sg} &= p_s - p_{\rm st} + p_{\rm st}(\text{new TC location}) = p_s + \tilde{p}_s, \quad (1)
\end{aligned}$$

where the increments due to the relocation are

$$\begin{aligned}
\tilde{u} &= u_t(\text{new TC location}) - u_t,\\
\tilde{v} &= v_t(\text{new TC location}) - v_t,\\
\tilde{\theta} &= \theta_t(\text{new TC location}) - \theta_t,\\
\tilde{\gamma} &= \gamma_t(\text{new TC location}) - \gamma_t,\\
\tilde{p}_s &= p_{\rm st}(\text{new TC location}) - p_{\rm st}. \quad (2)
\end{aligned}$$

The hydrostatic dry surface pressure μ_d and geopotential height Φ are also predicted variables in the WRF model, but cannot be directly included in the above relocation procedure because they should be diagnosed from θ, γ, and p_s (Skamarock et al. 2008). Otherwise, an unbalanced WRF initial state will be created, which violates the diagnostic relationship and causes the model to crash during the time integration. Once the surface pressure and water vapor mixing ratio increments are calculated, the μ_d increment can be computed by removing the moisture contribution from the surface pressure increment as in Eq. (3):

$$\tilde{\mu}_d = -\frac{\left(\tilde{p}_s - \mu_d \int_{0.0}^{1.0} \tilde{\gamma}\, d\eta\right)}{\int_{0.0}^{1.0} (1+\gamma)\, d\eta}. \quad (3)$$

The mass of the dry air in the column after the relocation is

$$\mu_{\mathrm{dg}} = \mu_d + \tilde{\mu}_d. \tag{4}$$

In the ARW-WRF forecast model, geopotential height is an important variable that links the vertical velocity and pressure in the prediction. The initialization of the Φ term must be computed from dry density ρ_d and μ_d by the diagnostic and hydrostatic equation:

$$\partial_\eta \Phi_h = -\frac{\mu_d}{\rho_d}. \tag{5}$$

The dry density ρ_d is related to pressure, temperature, and moisture, and is not trivial to derive ρ_d (see the appendix). Once the ρ_d after the relocation is obtained, the model-consistent Φ can be calculated by integrating Eq. (5).

The vortex relocation procedure is performed only when (i) the first-guess TC center is more than one grid distance away from the observed location, (ii) the maximum wind speed of the first-guess TC at $\eta = 0.85$ is greater than 15 m s^{-1}, (iii) the TC center is at least 300 km away from the lateral boundary, and (iv) there are no grid points with terrain height greater than 50 m within 150 km of the TC center. The terrain-height condition is imposed to avoid relocating a TC vortex that is distorted by high terrains. The high terrains near a TC center may affect the vortex relocation in three ways. The low-level wind distribution is greatly modified by the high terrains that the TC edge cannot be properly determined. The low-level TC circulation modified by the high terrains is no longer equivalent barotropic in the vertical that the TC edge determined at $\eta = 0.85$ may not be applicable to all levels. Finally, the large gradient of pressure, height, and temperature on η levels at a high terrain point may be relocated to a point with very different terrain height that creates imbalances in the relocated flow. The problem associated with the last effect may be improved by performing the vortex relocation on constant pressure levels through interpolating the first-guess fields to the pressure levels and then interpolating the relocation increments back to the η levels. However, the relocation on constant pressure levels cannot help the first two problems caused by the high terrains. In section 3b, a case of TC Jangmi approaching Taiwan is used to illustrate the necessity of imposing this high-terrain condition on the vortex relocation. The condition, however, is tunable that may be modified when the vortex relocation is applied at different areas. In cases a TC is near or over low terrain that the TC vortex can be properly determined, the terrain-height difference before and after the relocation may cause several hectopascals difference in the surface pressure. The terrain contamination on relocated surface pressure can be eliminated, as suggested by an anonymous reviewer, by relocating sea level pressure and then converting the sea level pressure back to surface pressure after the relocation. It is a good technique worthwhile trying. However, for all typhoons we are interested in East Asia, the complicated terrain prohibits such cases from existence. It is worth noting that there is often more than one TC in the WRF model domain. The previous relocation procedure is applied individually to each TC inside the model domain.

After the vortex relocation is performed, the WRF-3DVAR analysis (Barker et al. 2004) is used to assimilate the observational and bogus data with the new first guess. Its configuration is based on an incremental formulation to produce multivariate incremental analyses for surface pressure, wind, temperature, and relative humidity at the model grid points. The minimization of the incremental cost function is conducted in a preconditioned control variable space. The WRF-3DVAR has several background error statistics options for control variables. The "cv5" option, which we have adopted here, formulates physical-space control variables: stream-function, unbalanced velocity potential, unbalanced surface pressure, unbalanced temperature, and "pseudo" relative humidity. The background error covariance matrix allows for a separate definition of the vertical and horizontal correlation functions. A statistical regression is used to estimate background error cross covariance via the National Meteorological Center (NMC) method (Parrish and Derber 1992). An additional description of the 3DVAR system can be found in Barker et al. (2004).

For TC analysis at CWB, dynamically consistent bogus data are created near an observed TC to help the 3DVAR analysis in better defining TC structure. A new method different from that used in the NFS (Liou 2002) is developed for the WRF-3DVAR TC analysis. The method first removes the typhoon vortex from the first guess by a filtering procedure following Kurihara et al. (1993) to get environmental flow. It then implants an idealized vortex at the observed typhoon location with a wind profile proposed by Chan and William (1987) as

$$V(r) = V_m\left(\frac{r}{r_m}\right)\exp\left\{\frac{1}{b}\left[1-\left(\frac{r}{r_m}\right)^b\right]\right\}, \tag{6}$$

where V_m is the maximum wind, r_m is the radius of maximum wind, and factor b is the shape of outer wind profile. In Eq. (6), the V_m is directly from the observation and the r_m and b are iteratively computed by the nonlinear balance equation and hydrostatic equation,

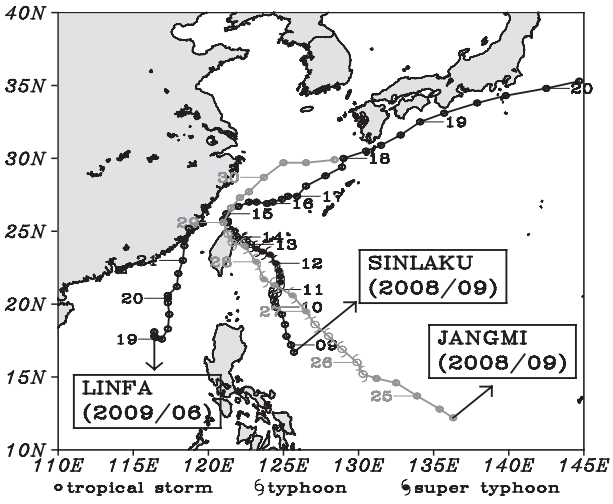

FIG. 1. CWB best-track positions for Typhoons Sinlaku, Jangmi, and Linfa plotted every 6 h with labels indicating 0000 UTC Sep 2008 for Sinlaku and Jangmi and 0000 UTC Jun 2009 for Linfa.

together with observed 15 m s^{-1} wind radius available from CWB forecasters, as follows:

$$\ln\left(\frac{15}{V_m}\frac{r_m}{r_{15}}\right) = \frac{1}{b}\left[1 - \left(\frac{r_{15}}{r_m}\right)^b\right], \tag{7}$$

$$\nabla^2\left[\varphi + \frac{1}{2}(\nabla\psi)^2\right] = \nabla\cdot[(f + \nabla^2\psi)\nabla\psi], \tag{8}$$

$$\ln P_s \approx \ln P + \frac{\varphi}{RT_a}, \tag{9}$$

where φ is the geopotential height of the bogusing vortex, ψ is the streamfunction, P is 1° area mean sea level pressure of environmental flow, T_a is the mean environmental surface temperature, R is the gas constant, r_{15} is the radius of 15 m s^{-1} wind, and P_s is the calculated sea level pressure of the typhoon. For a trial r_m in iteration, the parameter b is numerically computed by an advanced linear method following Fiorino and Elsberry (1989). The iteration is completed when P_s at the typhoon center is less than or equal to the observed central pressure of the typhoon, which is available from CWB forecasters. A gradually decreased wind profile is specified in the vertical to give a temperature structure with a warm core near 400 hPa. After the mass and wind fields of the bogusing vortex are determined, a normal model initialization is used to balance the total flow, which is environmental flow plus bogusing vortex. Moisture is assumed to be near saturated, 95% relative humidity, below 400 hPa and gradually reduced to 20% at the model top within the radius of maximum wind. The bogus data of sea level pressure, wind, temperature, and relative humidity derived from the above are constructed on 19 pressure levels between 1000 and 200 hPa at the TC center, 4 points at 0.5° and 8 points at each radius increased in every 1° from the TC center. Depending upon the size of the typhoon, there are 29 bogus data points within 3° of the typhoon center for smaller typhoons with $r_{15} \leq 200$ km and 37 bogus data points within 4° of the center for typhoons with $r_{15} > 200$ km. These bogus data are treated as observational data and assimilated in the WRF-3DVAR analysis as prior descriptions.

To examine the impact of the vortex relocation scheme on the ARW-WRF TC forecast, two sets of numerical experiments, with (WR) and without (NR) the vortex relocation, are conducted for 72-h forecasts with update cycles in the data assimilation. The experiments use the ARW-WRF forecast model with 45-km grid resolution and 222 by 128 grid points in the zonal and meridional directions, respectively. Three typhoons for which CWB issued warnings in 2008 and 2009, Sinlaku, Jangmi, and Linfa, are selected for the numerical experiments with a total of 70 forecast runs in each experiment set.

3. Results

a. *Synopsis of Typhoons Sinlaku, Jangmi, and Linfa*

Both Sinlaku and Jangmi reached super typhoon intensity before landfall on Taiwan in September 2008 (Fig. 1). Typhoon Sinlaku was named a tropical storm at 1800 UTC 8 September over the Philippines and moved north-northwestward along the edge of the subtropical high gradually intensifying. It made landfall about 0150 UTC 14 September at I-Lan in northeastern Taiwan and then weakened while approaching and passing over northern Taiwan. Typhoon Jangmi formed northwest of Guam on 24 September. As it moved persistently northwest during its first 4 days, its intensity increased gradually. Subsequently, Jangmi made landfall at I-Lan at 0740 UTC 28 September and left Taiwan near Tao-Yuan at 2020 UTC on the same day. After passing over Taiwan, Jangmi turned north-northeastward and dissipated over the ocean 2 days later.

On the other hand, Typhoon Linfa was a weaker storm with maximum wind less than 28 m s^{-1} for the whole lifetime in June 2009. It was almost stationary during the first day of its formation west to Philippines at 0600 UTC 18 June. Linfa moved north-northeastward for about 2 days and eventually dissipated over the Taiwan Strait around 1800 UTC 21 June when its center was just off the coast of Fujian province of China.

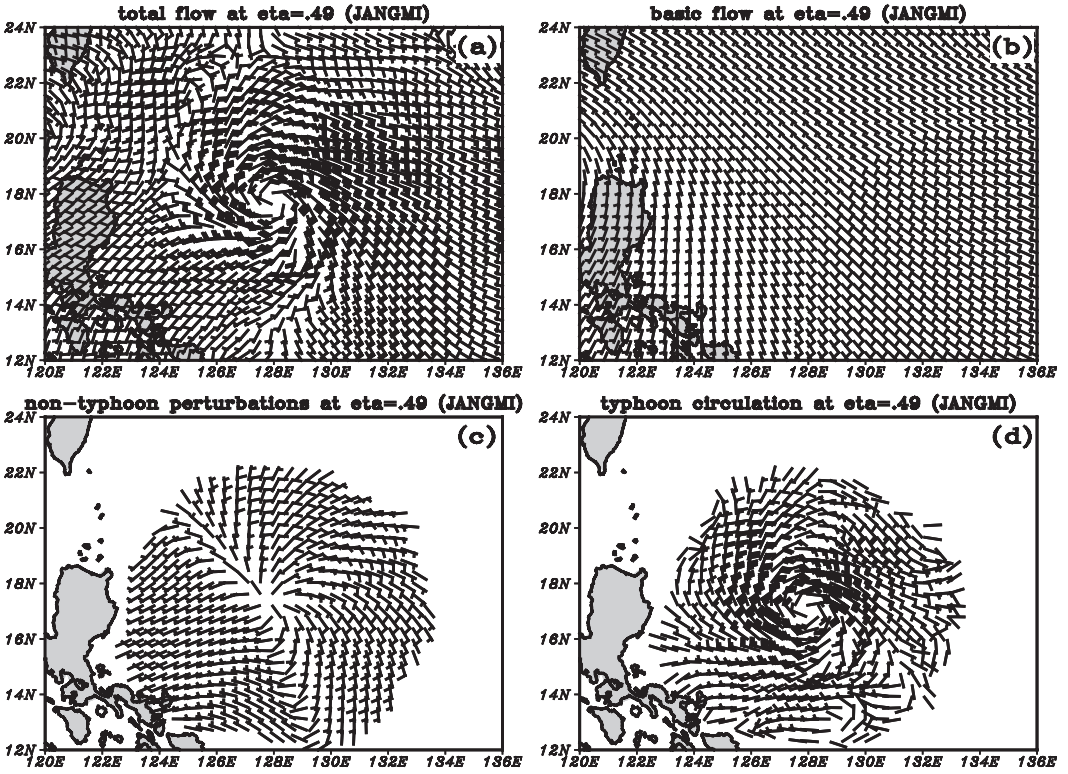

FIG. 2. Decomposition ($\eta = 0.49$) of Typhoon Jangmi at 1200 UTC 26 Sep 2008 for the vortex relocation (a) total flow, (b) basic flow, (c) nontyphoon perturbations, and (d) typhoon circulation.

b. Numerical experiments

The numerical experiments with (WR) and without (NR) the vortex relocation are all cold-started (using the NCEP GFS as a first guess) from 0600 UTC 8 September 2008 for Typhoon Sinlaku, 0000 UTC 24 September 2008 for Typhoon Jangmi, and 1800 UTC 17 June 2009 for Typhoon Linfa. For subsequent runs, each of the numerical experiments carries its own 6-h data assimilation cycle with the first guess for the 3DVAR analysis coming from the 6-h forecast of the previous run. Results after two update cycles (i.e., from 1800 UTC 8 September 2008 for Sinlaku, 1200 UTC 24 September 2008 for Jangmi, and 0600 UTC 18 June 2009 for Linfa) are used in the following studies. There are 37 runs (1800 UTC 8–17 September 2008) for Typhoon Sinlaku, 21 runs (1200 UTC 24–29 September 2008) for Typhoon Jangmi, and 12 runs (0600 UTC 18 June–0000 UTC 21 June 2009) for Typhoon Linfa.

1) ILLUSTRATIONS OF DECOMPOSITION AND VORTEX RELOCATION

One of the Typhoon Jangmi cases, 1200 UTC 26 September, is selected here to illustrate the vortex relocation procedure described in section 2 and its impact on the TC analysis. The vortex relocation scheme first decomposes the atmospheric flow around Typhoon Jangmi into TC circulation flow and environmental flow with the environmental flow consisting of basic flow and non-TC perturbations (Fig. 2). The relocated first guess is then obtained by relocating the TC circulation to the observed typhoon position and adding it back to the environmental flow. It is interesting to see that the environmental flow around the typhoon area is southeasterly, which is aligned with the typhoon's northwestward movement at this time as shown in Fig. 1. Meanwhile, the asymmetric structure of the TC circulation with weaker winds in the southeast quadrant (Fig. 2d) is similar to that in the total flow indicating that the asymmetric pattern is not from the environmental flow. Other vertical levels show similar results as those displayed here for the level $\eta = 0.49$ (about 500 hPa). The TC circulation shown in Fig. 2 clearly demonstrates that the model predicted vortex is very reasonable and realistic, which should be a basic requirement for the vortex relocation scheme to work properly. The model-predicted vortex is consistent with model dynamics and physics that may be in better balance than the TC vortex indirectly generated by other initialization methods.

A comparison of the perturbation dry air mass in the column μ'_d, which is an input to the first guess of the WRF 3DVAR analysis, before and after the relocation,

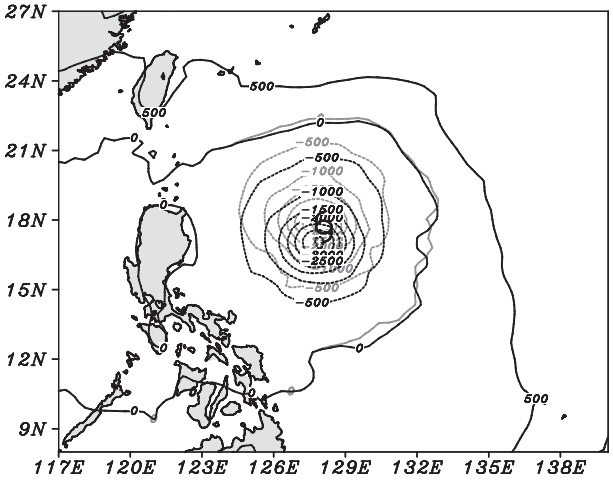

FIG. 3. The first guess of perturbation dry air mass in column (μ'_d) at 1200 UTC 26 Sep 2008 before (black) and after (gray) the vortex relocation scheme with the typhoon symbol indicating the observed position.

clearly shows significant modifications being made by the vortex relocation scheme on the μ'_d field (Fig. 3). The vortex relocation scheme moves the first-guess TC circulation to the north where the typhoon center was observed at 1200 UTC 26 September. Similar to the μ'_d field, the relocated wind field at $\eta = 0.85$ exhibits the northward displacement of the TC circulation to match the observed TC position (not shown). As a result, the vortex relocation scheme successfully relocates the TC circulation without generating discontinuity or sharp gradients. Other first guesses of the WRF 3DVAR analysis such as temperature, surface pressure, and relative humidity are also modified by shifting the TC circulation to match the observed TC position (not shown) as that for μ'_d and wind fields.

When a TC is too close to high terrains, the interaction between the TC circulation and terrains may distort the TC vortex that makes the vortex relocation inadequate. For example, when Typhoon Jangmi was moving toward Taiwan at 0000 UTC 28 September the blocking by Taiwan terrain distorts the typhoon circulation at $\eta = 0.97$ and $\eta = 0.85$ levels (Figs. 4a,b). Because of the difference in the degree of blocking by the central mountain ridge of Taiwan, the wind directions at the two levels were very different in the first and fourth quadrants. Therefore, the typhoon edge at $\eta = 0.97$ cannot be determined by the wind distribution at the $\eta = 0.85$ level. Furthermore, the distorted typhoon circulation is far from a vortexlike circulation that its edge cannot be properly determined by the criteria set for a vortex. In this Typhoon Jangmi case, the typhoon edge determined by the criteria is very irregular due to the upstream and

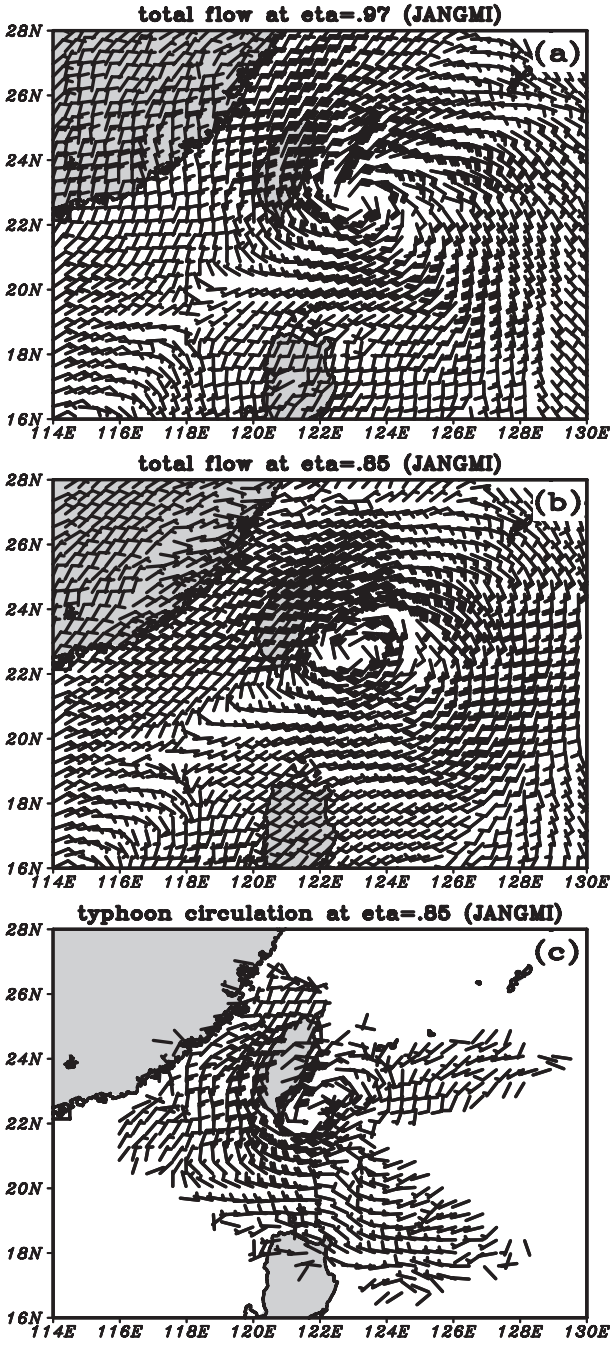

FIG. 4. Low-level wind distorted by Taiwan terrain as Typhoon Jangmi approaching Taiwan at 0000 UTC 28 Sep 2008 at (a) $\eta = 0.97$ level, (b) $\eta = 0.85$ level, and (c) extracted typhoon circulation at $\eta = 0.85$ level.

downstream blocking (Fig. 4c). If the irregular typhoon circulation is relocated to a new place, there will be large gradients near the edge of the relocated typhoon circulation causing unbalance in the relocated first guess. We skip the vortex relocation in this case.

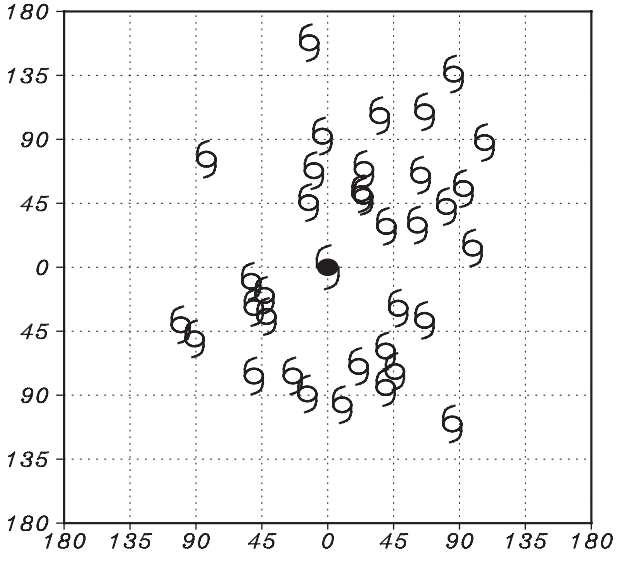

FIG. 5. Typhoon 6-h forecast positions (open typhoon symbols) relative to the observed position (closed typhoon symbol) for 35 cases that require the vortex relocation in the WR experiment (axis units in km).

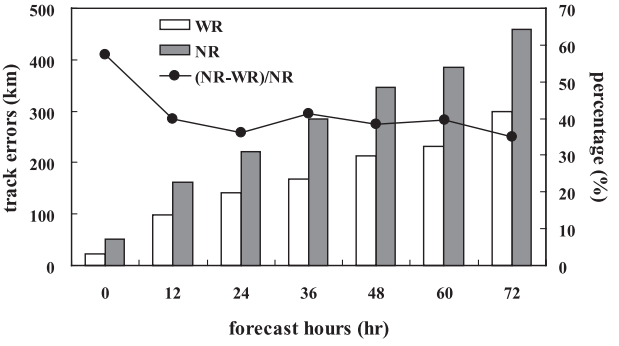

FIG. 6. Mean typhoon track errors for WR (white bars) and NR (shaded bars) experiments and the percentage of the mean track error reduction by the vortex relocation scheme (solid line) from 70 ARW-WRF forecasts.

2) STATISTICS AND TRACK COMPARISON

With the vortex relocation scheme described in section 2, the WR forecast runs can be classified into three categories: cases with terrain higher than 50 m within 150 km of the typhoon center, cases with the first-guess typhoon position error less than, and more than 1 grid distance. Out of the 70 cases, there are 18 cases in which the vortex relocation is skipped due to high terrain near the typhoon center, 17 cases that the vortex relocation is not needed since the position error is less than 1 grid distance, and 35 cases in which the vortex relocation is performed. As a result, 50% of all cases in the WR experiment need relocation of the typhoon circulation. However, if the topographical effect is excluded, the probability of requiring vortex relocation is about 67% in this ARW-WRF typhoon forecast experiment. This high percentage means that the 6-h track error of the ARW-WRF forecast is very likely larger than 45 km and the vortex relocation scheme plays an important role for the ARW-WRF typhoon initialization.

Figure 5 shows first-guess typhoon positions (open typhoon symbols) relative to the observed position (closed typhoon symbol) for the 35 cases that require the vortex relocation in the WR experiments. The relative typhoon positions appear in all quadrants but more concentrated in the first quadrant, indicating a northeastward bias in the 6-h track forecast. Since the vortex relocation scheme is not performed when the track error is less than 1 grid distance, there are no open typhoon symbols shown in Fig. 5 within a 45-km radius. It is surprising that the largest 6-h track error of the ARW-WRF forecast shown in Fig. 5 almost reaches 180 km.

The comparison of the mean track errors between the WR and NR experiments for the 70 forecasts reveals that the vortex relocation scheme significantly improves the ARW-WRF typhoon track forecast not only at initial time, but also throughout the whole 72-h forecast period (Fig. 6). In particular, the relocation scheme effectively improves the TC position error by more than 50% at the initial time and more than 34% during the rest of the forecast periods.

3) CASE OF 1800 UTC 26 SEPTEMBER

To demonstrate how the vortex relocation scheme may improve the typhoon track forecast, we select the Typhoon Jangmi forecast from 1800 UTC 26 September as an example to compare typhoon tracks and structures between the WR and NR experiments.

(i) Track and intensity

A comparison of 72-h track forecasts from these two experiments clearly shows a much better typhoon track forecast from the WR run starting at this time (Fig. 7). The track errors are 208, 95, and 312 km from the WR run and 275, 263, and 523 km from the NR run at 24-, 48-, and 72-h forecasts, respectively. In the NR experiment, the initial typhoon position was located 115 km northwest of the observed position, near the observed position 6 h later. The typhoon then took a very unrealistic southwestward movement at the beginning of the forecast and only turned back to move northwestward after 12 h. The anomalous initial movement may be explained by the broader and distorted typhoon circulation shown in the sea level pressure analysis of the NR experiment as compared with a tighter and circular typhoon circulation shown in the WR experiment (Fig. 8).

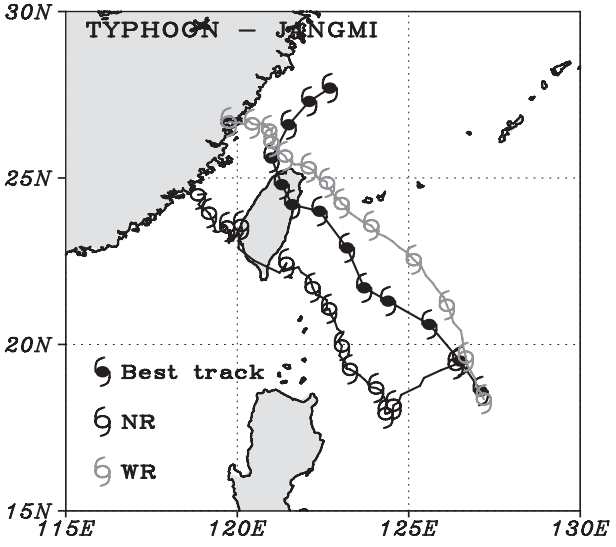

FIG. 7. Tracks of Typhoon Jangmi in every 6 h from the CWB best track (closed symbols), WR (gray open symbols), and NR (black open symbols) experiments for a 72-h forecast starting from 1800 UTC 26 Sep 2008.

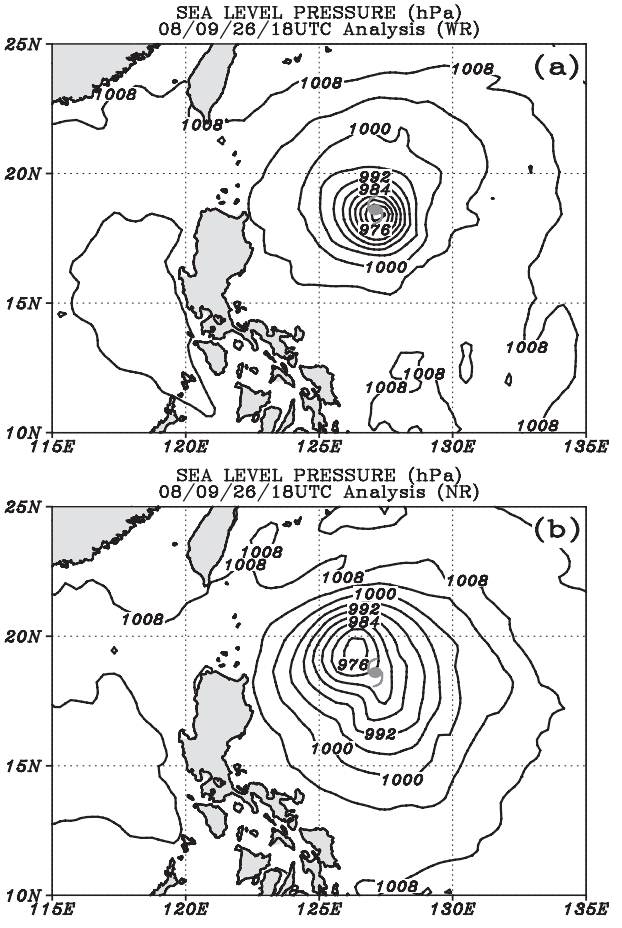

FIG. 8. The sea level pressure analysis from (a) WR and (b) NR experiments at 1800 UTC 26 Sep 2008 with the typhoon symbol indicating the observed position.

The sea level pressure analysis from the WR experiment at 1800 UTC 26 September is not only 8 hPa deeper than that from the NR experiment (i.e., 966 vs 974 hPa), but also much tighter in the TC circulation. The large distance between the typhoon centers in the observation and first guess of the NR experiment leads to an incorrect TC analysis with its center near the first-guess position while the southeastward extension of the cyclone shows the failure of the WRF 3DVAR in correcting the first guess due to such large errors. Since the bogus data are created around the observed TC position, the wind in the bogus soundings near the incorrectly analyzed TC center is northeasterly as they are located northwest to the observed TC position. The analyzed northeasterly wind near the analyzed TC center acts as a strong northeasterly steering flow that causes the southwestward movement at the initial time (see Fig. 7). The distorted typhoon circulation is adjusted to be consistent with the dynamics and physics of the model during the early integration period, which coincides with the large track errors during the first 12 h. There are many cases in the NR experiment having an anomalous track during the initial adjustment due to errors in analyzing TC centers and steering flows. With the vortex relocation scheme, the TC position error is corrected in the first guess and less change is needed for the 3DVAR analysis in blending the first guess with observations.

The vortex relocation scheme also has impacts on the analyzed typhoon vertical structure. Figure 9 shows an east–west vertical cross section of potential temperature and relative humidity fields cutting across the analyzed typhoon center. The potential temperature field shows the presence of a trough around the typhoon center associated with the stronger typhoon structure in the WR experiment with the relocation. Meanwhile, the relative humidity exhibits the well-developed structure in both the horizontal and vertical with values close to 100% within the typhoon circulation. On the other hand, a less-organized typhoon structure is shown in the NR experiment without the relocation with double deep troughs of the potential temperature at low levels and dry areas at midlevels. Therefore, based on the Typhoon Jangmi case, the vortex relocation scheme has significant impacts not only on the typhoon track forecast, but also on the dynamic and thermodynamic vortex structure.

(ii) Impacts of bogus data on TC initialization

The large difference between the bogus data and first guesses causes an unrealistic analysis and anomalous initial track in this and other cases. We do not consider it

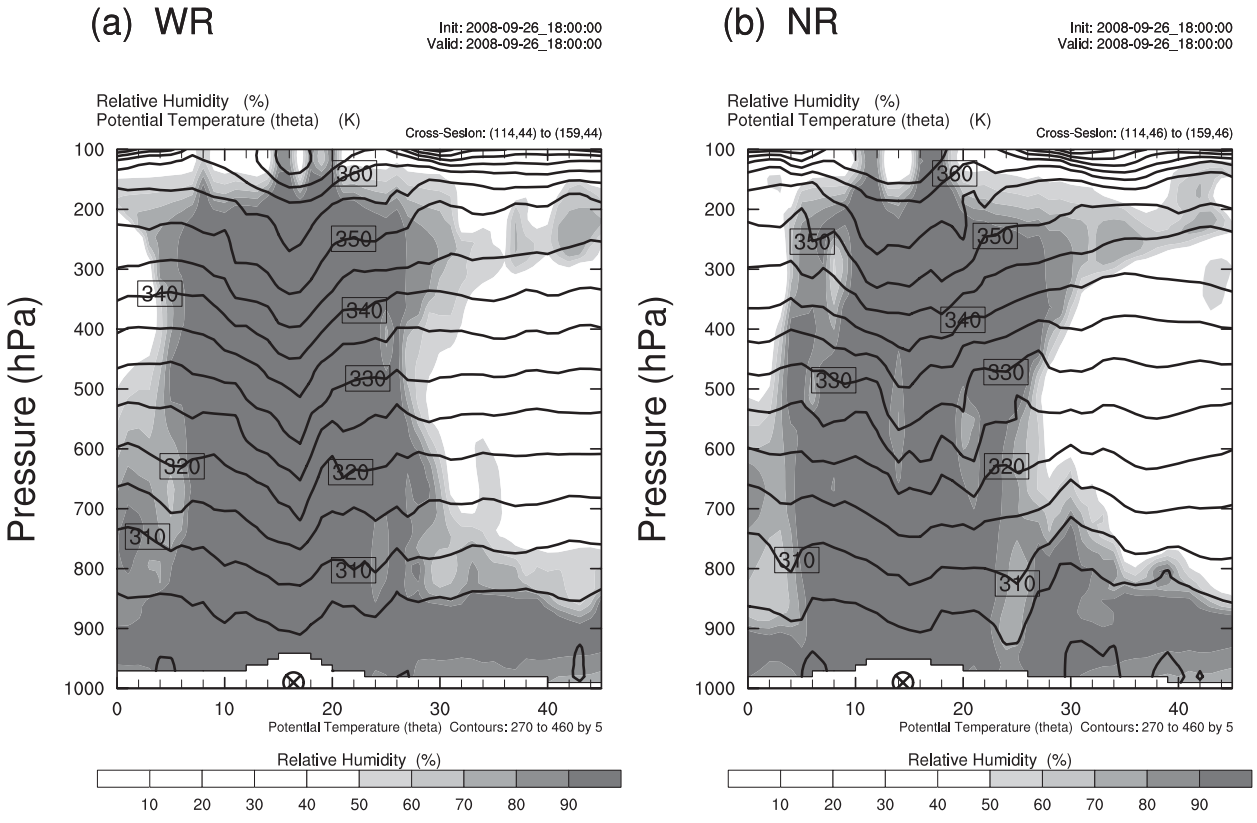

FIG. 9. Zonal cross section of initial potential temperature (black lines) and relative humidity (shaded) cutting through the typhoon center (open circle with a cross symbol) from (a) WR and (b) NR experiments at 1800 UTC 26 Sep 2008. The contour intervals are 5 K for potential temperature and 10% for relative humidity.

as a bad consequence of using bogus data. Many studies (Serrano and Undén 1994; Xiao et al. 2009) point out the essential need for bogus data in variational assimilation. Because conventional observations are too sparse to improve the typhoon forecast, bogus data are often able to improve forecasting skill for typhoon position and intensity. In addition, agencies that bogus a synthetic vortex or synthetic observations to initiate numerical typhoon forecast models include the Met Office (UKMO; Heming and Radford 1998), the GFDL (Kurihara et al. 1995), the Tropical Cyclone-Limited Area Prediction System (TC-LAPS) developed at the Australian Bureau of Meteorology Research Centre (Davidson and Weber 2000), and the Coupled Ocean–Atmosphere Mesoscale Prediction System (COAMPS) at the Naval Research Laboratory (Liou 2002). Bogus data, which improve the initial typhoon structure according to a typhoon conceptual model, can lead to significant improvement of the typhoon forecasting skill in global and regional models. In this study, despite the 45-km resolution that may not simulate realistic typhoon intensity, bogus data are able to provide the well-developed structure in the typhoon initialization.

To examine the relative roles of vortex relocation and bogus data in the WRF-3DVAR TC analysis, we have conducted experiments to test WRF-3DVAR TC analysis without bogus data. Figure 10 shows a typical example of the track forecast comparison for the WR and NR experiments with and without bogus data for TC initialization. Without bogus data, the track forecasts are significantly different from those with bogus data in the both experiments. The impact of the bogus data on the track forecast is mixed in the early periods with clearly improvement in the later periods after 36 h of the forecast. The track errors at 24-, 48-, and 72-h forecasts without the bogus data are 23, 215, and 512 km from the WR run and 233, 290, and 673 km from the NR run, respectively. Significant improvement in the initial track forecast of the NR experiment without the bogus data indicates that the bogus data enhance the distorted typhoon circulation when the position of the first-guess typhoon is not correct (Fig. 8b versus Fig. 11b). On the other hand, after the typhoon position is corrected by the vortex relocation, the bogus data help WRF-3DVAR to get a deeper and tighter typhoon circulation (Fig. 8a versus Fig. 11a) that results in the best track

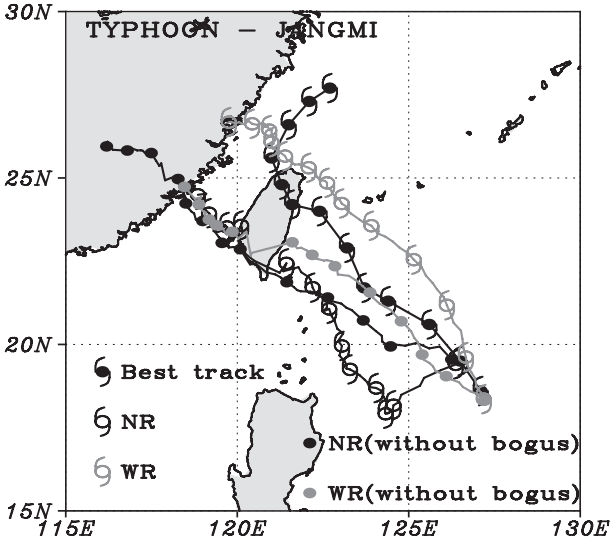

FIG. 10. As in Fig. 7, but adding tracks for the WR (gray closed circles) and NR (black closed circles) experiments without bogus data.

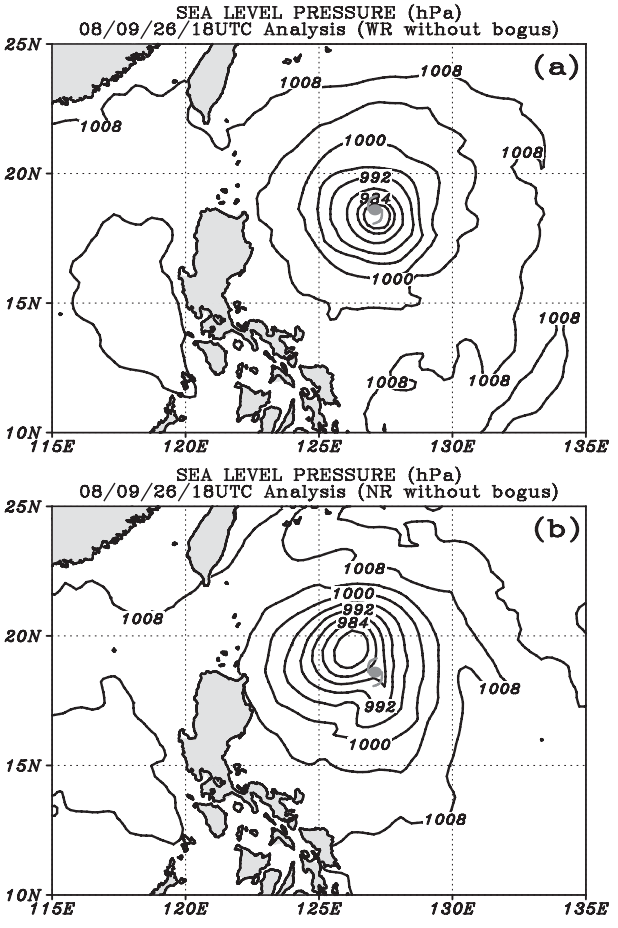

FIG. 11. As in Fig. 8, but for the (a) WR and (b) NR experiments without bogus data.

(312-km track error in 72-h forecast) and best intensity forecast (Fig. 12). Although, with 45-km grid resolution, the sea level pressure is much higher than the corresponding observation throughout the forecast periods in these experiments, the model is able to capture the evolution of typhoon intensity in the WR experiment with bogus data, especially the weakening before landfall at the 36-h forecast. In summary, with the vortex relocation, the bogus data significantly improve the intensity forecast in all forecast periods but improve the track forecast mainly at the later periods. Without the vortex relocation, on the other hand, the bogus data make little impact on the intensity forecast and degrade initial track forecast by making the initial typhoon circulation even more distorted. It is worth noting that the above experiments are performed at one time using same first-guess fields for the analysis. The impacts of bogus data on the TC analysis and forecast will be much more profound in update cycle runs when the data influence is accumulated through the cycles.

(iii) Relative impacts of model grid resolution

Wang (2001) demonstrated that a high-resolution model has the capability of simulating tropical cyclones. To better examine the impact of the vortex relocation on the intensity forecast, we have conducted a higher resolution experiment using nested grids of 15- and 5-km grid spacing with 183 × 195 and 267 × 273 grid points, respectively. The first-guess fields are horizontally interpolated from the 45-km resolution fields. The track forecast of the 5-km resolution run shows similar characteristics to that of 45-km resolution, in which the track is close to the observation in the WR experiment and southward movement in the NR experiment (Fig. 13). However, the typhoon intensity is much deeper in the 5-km resolution (Fig. 14) than that in the 45-km resolution. Furthermore, in case with the vortex relocation, the higher-resolution typhoon vortex is much tighter (Fig. 14a); while in case without the vortex relocation, the higher-resolution typhoon circulation is even more distorted with two low centers (Fig. 14b). With the higher resolution, the intensity forecast is closer to the observation and significant improvement is achieved by the vortex relocation in the first 36-h forecast (Fig. 15). In later periods, the intensity forecast comparison is complicated by the track error that typhoon and land interaction is different between the two experiments. The high-resolution WRF forecast confirms that the WRF-3DVAR analysis cannot correct the large TC position error in the background even with high-resolution grids and many bogus data around the TC, and the bogus data are important in improving the initial TC intensity. It also demonstrates that the better definition of the initial

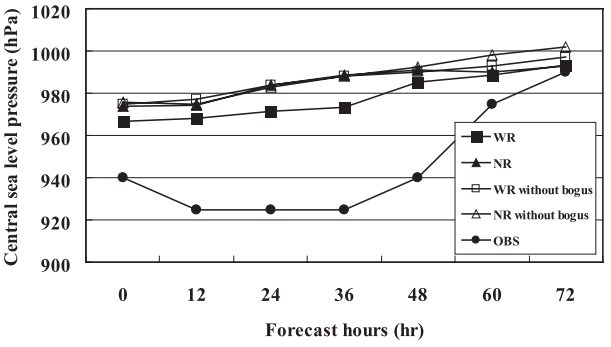

FIG. 12. Time evolution of the central sea level pressure of Typhoon Jangmi from CWB analyses (closed circles), the WR (closed boxes), and NR (closed triangles) experiments with bogus data, and the WR (opened boxes) and NR (opened triangles) experiments without bogus data.

vortex is a key reason for the improvements of typhoon track and intensity prediction in this case.

4) SHAPE COMPARISON

As shown by the Typhoon Jangmi forecast from 1800 UTC 26 September 2009 in the NR experiment, a large initial track error may be generated by a distorted typhoon circulation that is inconsistent with the model dynamics and physics. To better demonstrate this effect, we compare 1000-hPa contours of sea level pressure analyses around the analyzed typhoon centers between the WR and NR experiments (Fig. 16). Forty cases, excluding those with high terrain near the typhoon centers, are selected for this comparison. The 1000-hPa contours from the WR experiment are circular and located within 450 km from the typhoon centers (Fig. 16a). However, different results with irregular

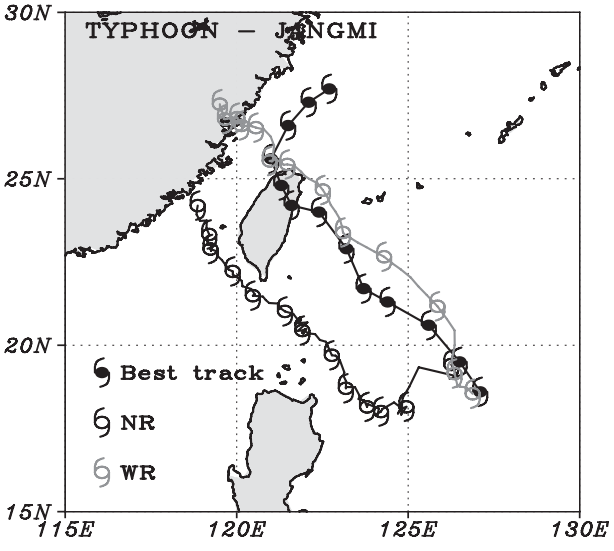

FIG. 13. As in Fig. 7, but for 5-km resolution forecast.

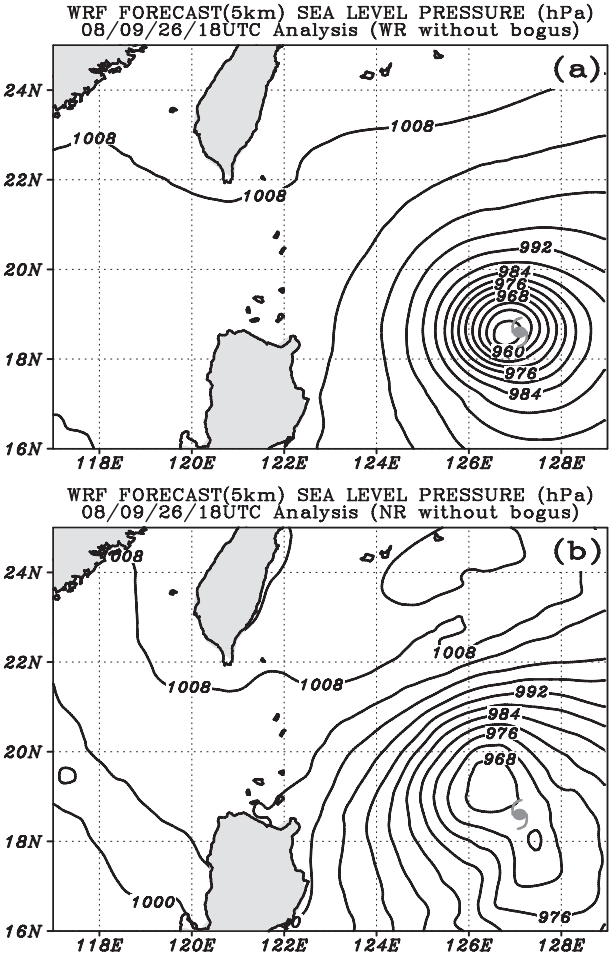

FIG. 14. As in Fig. 8, but for 5-km resolution analysis.

shape and wider-spread 1000-hPa contours are shown in the sea level pressure analyses from the NR experiment (Fig. 16b). To quantify the shape difference in the sea level pressure analyses between the experiments, we fit each 1000-hPa contour to an ellipse and compute the length of its axes in the x-(a) and y-(b) grid directions (Fig. 17). Because typhoons in the experiments are located at low latitudes, the map scale factor could be neglected here. Therefore, the eccentricity ε of analyzed sea level pressure is calculated from a and b as

$$\varepsilon = \sqrt{1 - \left(\frac{b}{a}\right)^2} \quad \text{if} \quad a \geq b, \quad \text{and}$$

$$\varepsilon = \sqrt{1 - \left(\frac{a}{b}\right)^2} \quad \text{if} \quad a < b.$$

The range of the eccentricity is $0 < \varepsilon < 1$ with $\varepsilon = 0$ for a circle. The averaged eccentricity from the WR and NR experiments are 0.33 and 0.5, respectively. The result

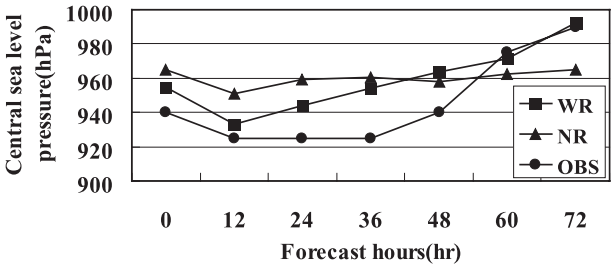

FIG. 15. As in Fig. 12, but for 5-km resolution forecast with bogus data.

indicates that the averaged 1000-hPa contour of the analyzed sea level pressure from the WR experiment tends to be more circular than that from the NR experiment. The larger ε value represents elongated typhoon structure from the NR experiment, which is another parameter demonstrating the distorted typhoon circulation in the analysis. The scatter diagram of parameters a and b from the two experiments shows that the parameters are confined near a straight line in the WR experiment while they are scattered around in the NR experiment (Fig. 18). The correlation coefficient to the regression line is 0.84 for the WR experiment and 0.41 for the NR experiment. The low correlation to the regression line represents incoherent typhoon circulation analyses from the NR experiment, which is another way of indicating the irregular typhoon circulation in the analysis. The outer spread points in the a and b scatter diagram represent cases with more ellipselike initial typhoon structure that requires large adjustment in the early forecast periods for consistency with the dynamics and physics of the model so that their track forecast errors will be larger. To support this assertion, we separate cases in the NR experiment according to the mean (1.08) and standard deviation (0.25) of b/a into two groups, within and beyond one standard deviation (Fig. 19). There are 37 cases with $0.83 \leq b/a \leq 1.33$ and 15 cases with $b/a > 1.33$ or $b/a < 0.83$. The mean track error comparison clearly shows that the cases with more ellipselike initial typhoon structure give much worse typhoon track forecasts than those with more circular initial structure (Fig. 20). The difference in the track forecast errors increases with forecast time and reaches 60% at 72 h. As we have demonstrated earlier, the distorted and elongated initial typhoon circulation is a result of a large position error in the first guesses with which the WRF 3DVAR is unable to completely correct. The vortex relocation scheme fixes the position error in the first guesses and helps 3DVAR in providing a more circular and stronger initial typhoon circulation.

4. Conclusions

The WRF model is a well-developed mesoscale forecast and data assimilation system that is designed to advance atmospheric research and operational prediction. However, tropical cyclones may not be properly initialized yet in WRF due to TC position errors in the first-guess fields. We have proposed a method of improving the TC initialization and hence TC forecasting skill for the ARW-WRF model by relocating the first-guess TC position to its observed location. The vortex relocation scheme is evaluated using 70 forecasts for Typhoons Sinlaku (2008), Jangmi (2008), and Linfa (2009) for which CWB issued typhoon warnings.

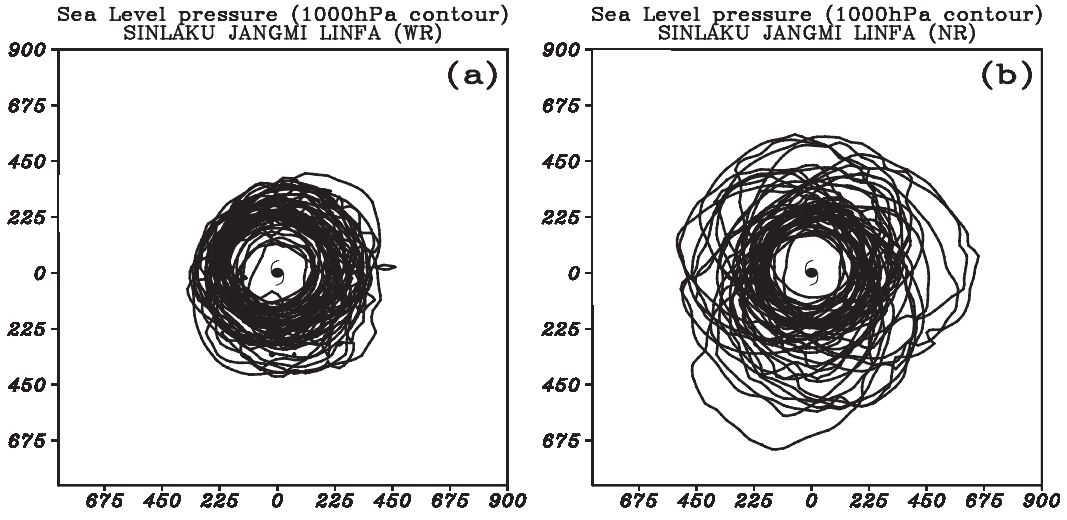

FIG. 16. 1000-hPa contours of sea level pressure analyzed relative to typhoon center (typhoon symbol) from 52 cases of (a) WR and (b) NR experiments (axis units in km).

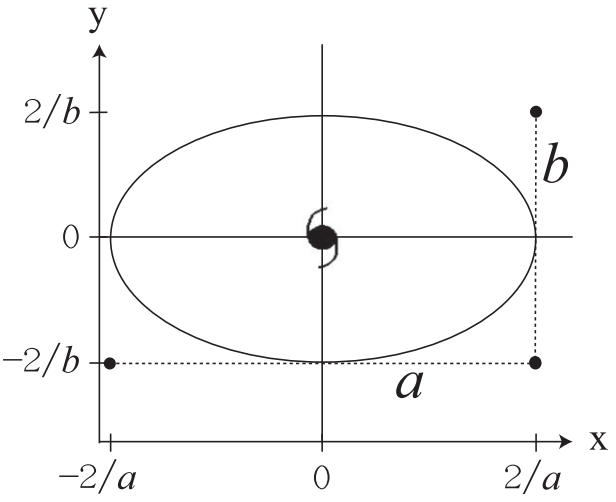

FIG. 17. Diagram showing the conceptual model for computing the axes (a and b) of a typhoon center fitted to an ellipse.

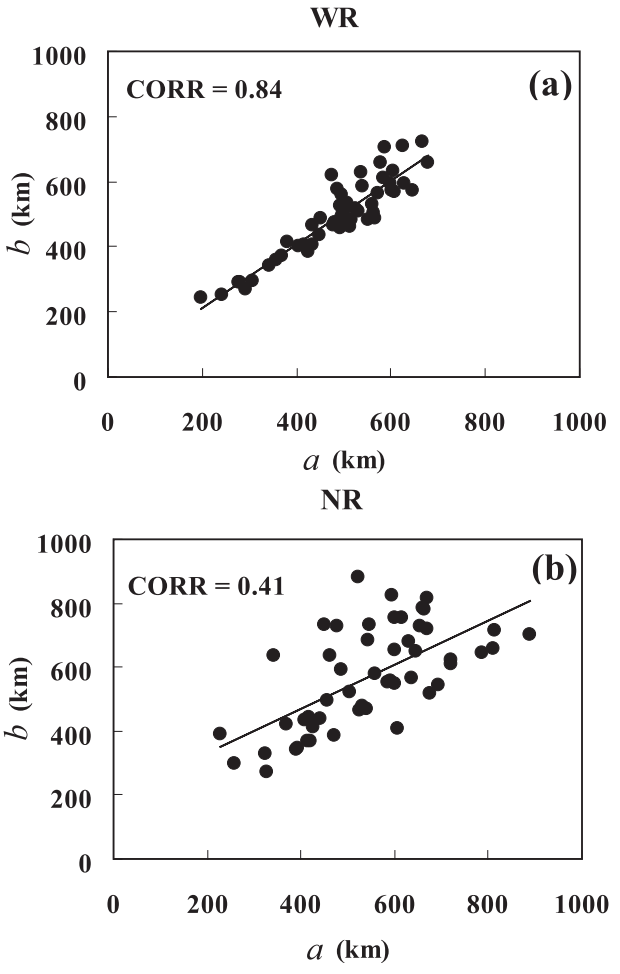

FIG. 18. Scatter diagram of the a and b axes fitted for typhoons in the (a) WR and (b) NR experiments with 0.84 and 0.41 correlation coefficients associated with the linear regression lines for the WR and NR experiments, respectively.

The vortex relocation scheme decomposes the atmospheric flow of the first guess into a TC circulation and environmental flow, while the environmental flow consists of the basic flow and non-TC perturbations. The TC circulation is relocated to match the observed TC position and then is added back to the environmental flow to form an improved first guess for the WRF 3DVAR analysis. The comparison between first-guess fields before and after the relocation shows that the relocation scheme successfully moves the TC circulation to a correct position without generating discontinuities or sharp gradients. The improved first guess results in stronger, tighter, and more realistic initial TC circulation from the WRF 3DVAR analysis.

Based on the vortex relocation experiments with and without the relocation procedure for Typhoons Jangmi, Sinlaku, and Linfa, a considerably high proportion (67% of the cases) requires typhoon relocation while eliminated the topographical effect. As the vortex relocation scheme effectively removes the typhoon position error from the first guess, the typhoon track forecast is considerably improved for all forecast periods. In particular, it eliminates distorted typhoon circulations and reduces the model dynamical and physics adjustment during the early forecast periods by providing a proper first guess of the initial typhoon circulation and position. The dynamic and thermodynamic structures of the typhoon circulation are better analyzed with the vortex relocation and the initial typhoon position agrees better with the observed typhoon position even in the process of data assimilation with bogus data. Similar to the horizontal structure, the thermodynamic vertical structure is better analyzed with the vortex relocation scheme as well. Overall, with the vortex relocation, large errors in the first-guess fields due to the position error are eliminated and the analyzed typhoon circulation is much more reasonable without distorted centers. It has been speculated that the failure of TC analysis by objective methods comes from not enough model resolution or observation data. Our results show that the difficulty may come from the poor first guess, in which the analysis method is not able to correct the position error of the first guess in spite of high resolution and many observations near the TC center.

Numerical experiments with and without bogus data demonstrate that the bogus data significant improves the typhoon intensity analysis when the typhoon position is corrected by the vortex relocation. On the other hand, without the vortex relocation, the bogus data cannot correct the position error and may make the distortion of the TC circulation even worse in the analysis. The high-resolution experiment confirms the positive impact of the vortex relocation on the intensity forecast.

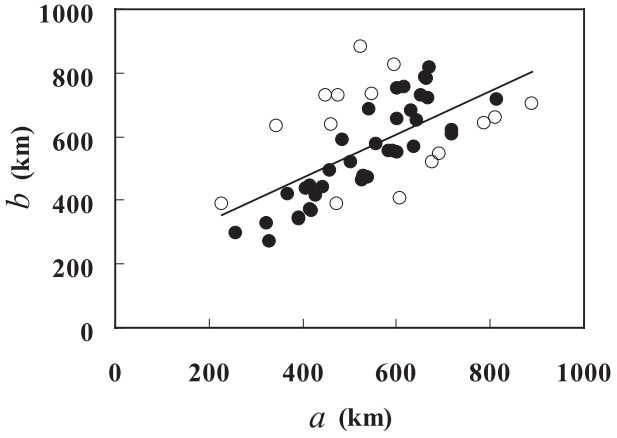

FIG. 19. As in Fig. 18b, but for $0.83 \le b/a \le 1.33$ cases plotted with closed circles and the other cases with open circles.

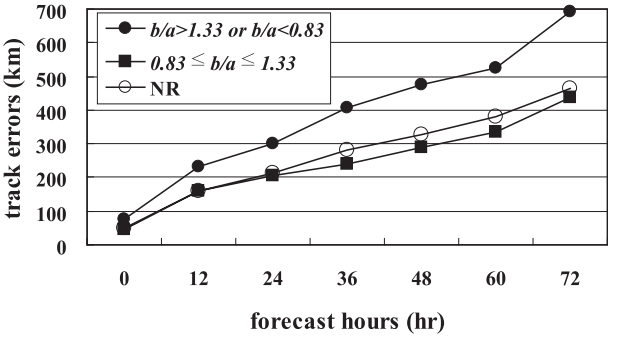

FIG. 20. Mean typhoon track errors from the NR experiment for all cases (open circles), cases with $0.83 \le b/a \le 1.33$ (solid boxes), and cases with $b/a > 1.33$ or $b/a < 0.83$ (closed circles).

The difference between the two experiments is quantified by comparing sea level pressure analyses. The comparison demonstrates that larger track errors may come from a distorted initial typhoon circulation when the vortex is not relocated. In an ellipse fitting analysis, the sea level pressure analyses without vortex relocation show a more ellipselike typhoon circulation with larger eccentricity when compared with sea level pressure analyses with relocation. Without the vortex relocation, the analyzed sea level pressure is often irregular in shape as shown by wide spread in the scatter diagram of the ellipse fitting. Larger track forecast errors are proven to be associated with cases at outer areas of the spread. In those cases, a distorted initial typhoon circulation is analyzed and a wrong steering flow acts on the incorrect typhoon center that causes an anomalous initial movement with large adjustment for consistency with model dynamics and physics.

As the vortex relocation scheme proposed in this paper can improve the first guess to avoid distorted TC circulations analyzed by the WRF 3DVAR, our study suggests that TC forecasts by the WRF model with update cycles should include the proposed vortex relocation scheme in the data assimilation procedure. It is also recommended for operational consideration as well.

Acknowledgments. This study was financially supported by the National Science Council of the R.O.C. under Grants NSC96-2625-Z-052-003 and NSC97-2625-M-052-002; and (for the second author) by the Office of Naval Research through Program PE-0602435N. The authors would also like to thank Dr. Ying-Hwa (Bill) Kuo, Dr. Jim Bresch, and the anonymous reviewers for their constructive comments and suggestions on the manuscript.

APPENDIX

Calculation of Geopotential Height in the TC Relocation Scheme

To compute the geopotential height Φ_g after the TC relocation, we need first to obtain the pressure increment $\tilde{p}$ and dry density ρ_d from the increments $\tilde{\theta}$ and $\tilde{\gamma}$ in Eq. (2) and $\tilde{\mu}_d$ in Eq. (3). The geopotential height Φ_g can then be calculated by integrating Eq. (5). The detailed procedure is stated in the following sections.

a. Calculation of the pressure p before the TC relocation

Since, the three-dimensional pressure p before the TC relocation is not available from the WRF input file, we need to compute the pressure p using the following equation:

$$p = p_0(R_d\theta_v/p_0\alpha_d)^{\kappa}, \tag{A1}$$

where R_d is the gas constant for dry air, p_0 is a reference pressure (typically 1000 hPa), θ_v is virtual potential temperature, $\theta_v = \theta(1+1.61\gamma)$, α_d is dry specific volume, and $\kappa = c_p/c_v$. The dry specific volume α_d consists of the base state $\overline{\alpha_d}$ and perturbation α'_d (i.e., $\alpha_d = \overline{\alpha_d} + \alpha'_d$). The base specific volume $\overline{\alpha_d}$ can be calculated from $\overline{\mu_d}$, while the perturbation α'_d can be calculated from $\overline{\alpha_d}$, $\overline{\mu_d}$, μ'_d, and Φ' as

$$\alpha'_d = -\frac{1}{\overline{\mu_d}}(\overline{\alpha_d}\mu'_d + \partial_\eta\Phi'). \tag{A2}$$

b. Calculation of the pressure increment $\tilde{p}$ after the TC relocation

The relation between the pressure perturbation p' and the variables μ_d and γ can be written as

$$dp' = \mu'_d(1+\gamma)\,d\eta + \gamma\overline{\mu_d}\,d\eta. \tag{A3}$$

Since the total pressure is defined as $p = \overline{p} + p'$ and the base state $\overline{p}$ is a constant in time, the increment $\tilde{p}$ is equal to the increment of the pressure perturbation p' (i.e., $\tilde{p} = \tilde{p}'$). To compute the pressure increment $\tilde{p}$, we linearize Eq. (A3) to be

$$d\tilde{p} = [\tilde{\mu}_d'(1 + \gamma) + \mu_d'\tilde{\gamma}]\, d\eta + \tilde{\gamma}\overline{\mu_d}\, d\eta.$$

With $\tilde{\mu}_d' = \tilde{\mu}_d$, we can rewrite the previous equation as

$$d\tilde{p} = [\tilde{\mu}_d(1 + \gamma) + \mu_d\tilde{\gamma}]\, d\eta. \tag{A4}$$

The three-dimensional pressure increment $\tilde{p}$ can then be obtained by vertically integrating the linear Eq. (A4) from the model top level to the bottom level using the $\tilde{\mu}_d$ computed from Eq. (3) and $\tilde{\gamma}$ computed from Eq. (2).

c. *Calculation of the dry density ρ_{dg} after the TC relocation scheme*

By the definition of the potential temperature and dry air state equation, the dry density ρ_d can be calculated as follows:

$$\rho_d = \frac{p - e}{R_d T} = \frac{p\left(1 - \dfrac{e}{p}\right)}{R_d T} = \frac{p\left(1 - \dfrac{R_v}{R_d}\gamma\right)}{R_d\theta\left(\dfrac{p}{p_0}\right)^{R_d/c_p}}$$

$$\cong \frac{p}{R_d\theta\left(\dfrac{p}{p_0}\right)^{R_d/c_p}\left(1 + \dfrac{R_v}{R_d}\gamma\right)}, \tag{A5}$$

where e is the water vapor pressure and c_p is the specific heat of dry air at constant pressure. Since the after relocation variables θ_g and γ_g can be calculated from Eq. (1) and p_g ($=p + \tilde{p}$) can be calculated from Eq. (A1) and Eq. (A4), the dry density after the relocation ρ_{dg} can be obtained from Eq. (A5) by replacing θ, γ and p with the after relocation variables θ_g, γ_g, and p_g.

d. *Derivation of the geopotential height Φ_g after the TC relocation*

The hydrostatic geopotential height after the Φ_h can be diagnosed as

$$\partial_\eta \Phi_h = -\mu_{\mathrm{dg}}/\rho_{\mathrm{dg}}. \tag{A6}$$

By vertically integrating Eq. (A6) from the bottom level up to the top level, we can obtain the three-dimensional hydrostatic geopotential height Φ_h.

The input field of Φ before relocation may contain both hydrostatic and nonhydrostatic parts. To keep the nonhydrostatic part from the input field, the nonhydrostatic geopotential height Φ_{nh} can be obtained by computing the difference, before the relocation, between the total geopotential height (base state and perturbation) and the hydrostatic part geopotential height. Finally, the geopotential height Φ_g is composed of hydrostatic and nonhydrostatic geopotential height as $\Phi_g = \Phi_h + \Phi_{\mathrm{nh}}$.

REFERENCES

Barker, D. M., W. Huang, Y.-R. Guo, A. J. Bourgeois, and Q. N. Xiao, 2004: A three-dimensional variational data assimilation system for MM5: Implementation and initial results. *Mon. Wea. Rev.,* **132,** 897–914.

Barnes, S. L., 1994: Application of the Barnes objective analysis scheme. Part I: Effects of undersampling, wave position, and station randomness. *J. Atmos. Oceanic Technol.,* **11,** 1433–1448.

Bender, M. A., I. Ginis, R. Tuleya, B. Thomas, and T. Marchok, 2007: The operational GFDL coupled hurricane–ocean prediction system and a summary of its performance. *Mon. Wea. Rev.,* **135,** 3965–3989.

Chan, J. C.-L., and R. T. Williams, 1987: Analytical and numerical studies of the beta-effect in tropical cyclone motion. Part I: Zero mean flow. *J. Atmos. Sci.,* **44,** 1257–1265.

Davidson, N. E., and H. C. Weber, 2000: The BMRC high resolution tropical cyclone prediction system: TC-LAPS. *Mon. Wea. Rev.,* **128,** 1245–1265.

Davis, C. A., and S. Low-Nam, 2001: The NCAR-AFWA tropical cyclone bogussing scheme. Air Force Weather Agency (AFWA) Rep., 12 pp. [Available online at http://www.mmm.ucar.edu/mm5/mm5v3/tc-bogus.html.]

——, and Coauthors, 2008: Prediction of landfalling hurricanes with the advanced hurricane WRF model. *Mon. Wea. Rev.,* **136,** 1990–2005.

Fiorino, M., and R. L. Elsberry, 1989: Some aspects of vortex structure related to tropical cyclone motion. *J. Atmos. Sci.,* **46,** 975–990.

Fujita, T., 1952: Pressure distribution within a typhoon. *Geophys. Mag.,* **23,** 437–451.

Grell, G. A., and D. Devenyi, 2002: A generalized approach to parameterizing convection combining ensemble and data assimilation techniques. *Geophys. Res. Lett.,* **29,** 1693, doi:10.1029/2002GL015311.

Heming, J. T., and A. M. Radford, 1998: The performance of the United Kingdom Meteorological Office Global Model in predicting the tracks of Atlantic tropical cyclones in 1995. *Mon. Wea. Rev.,* **126,** 1323–1331.

Hong, S.-Y., Y. Noh, and J. Dudhia, 2006: A new vertical diffusion package with an explicit treatment of entrainment processes. *Mon. Wea. Rev.,* **134,** 2318–2341.

Jankov, I., W. A. Gallus Jr., M. Segal, B. Shaw, and S. E. Koch, 2005: The impact of different WRF model physical parameterizations and their interactions on warm season MCS rainfall. *Wea. Forecasting,* **20,** 1048–1060.

Kurihara, Y., M. A. Bender, R. E. Tuleya, and R. J. Ross, 1990: Prediction experiments of Hurricane Gloria (1985) using a multiply nested movable mesh model. *Mon. Wea. Rev.,* **118,** 2185–2198.

——, ——, and R. J. Ross, 1993: An initialization scheme of hurricane models by vortex specification. *Mon. Wea. Rev.,* **121,** 2030–2045.

——, ——, R. E. Tuleya, and R. J. Ross, 1995: Improvements in the GFDL hurricane prediction system. *Mon. Wea. Rev.,* **123,** 2791–2801.

Liou, C.-S., 2002: High-resolution numerical modeling on tropical cyclone structure and track. *Weather and Climate Modeling,* S.V. Singh, S. Basu, and T. N. Krishnamurti, Eds., New Age International (P) Limited, 198–208.

——, 2004: Improving forecast of rainfall and strong wind associated with typhoons approaching Taiwan. CWB Rep. CWB93-3M-01, 2-24, 318 pp.

Liu, Q., T. Marchok, H. Pan, M. Bender, and S. Lord, 2000: Improvements in hurricane initialization and forecasting at NCEP with global and regional (GFDL) models. NCEP/EMC Tech. Procedures Bull. 472, 7 pp. [Available online at http://205.156.54.206/om/tpb/472.htm.]

——, S. Lord, N. Surgi, Y. Zhu, R. Wobus, Z. Toth, and T. Marchok, 2006: Hurricane relocation in global ensemble forecast system. Preprints, *27th Conf. on Hurricanes and Tropical Meteorology,* Monterey, CA, Amer. Meteor. Soc., P5.13.

Lord, S. J., 1991: A bogussing system for vortex circulations in the National Meteorological Center Global Forecast Model. Preprints, *19th Conf. on Hurricanes and Tropical Meteorology,* Miami, FL, Amer. Meteor. Soc., 328–330.

Moeng, C.-H., J. Dudhia, J. B. Klemp, and P. P. Sullivan, 2007: Examining two-way grid nesting for large eddy simulation of the PBL using the WRF model. *Mon. Wea. Rev.,* **135,** 2295–2311.

Parrish, D. F., and J. C. Derber, 1992: The National Meteorological Center's spectral statistical-interpolation analysis system. *Mon. Wea. Rev.,* **120,** 1747–1763.

Pu, Z.-X., and S. A. Braun, 2001: Evaluation of bogus vortex techniques with four-dimensional variational data assimilation. *Mon. Wea. Rev.,* **129,** 2023–2039.

Serrano, E., and P. Undén, 1994: Evaluation of a tropical cyclone bogusing method in data assimilation and forecasting. *Mon. Wea. Rev.,* **122,** 1523–1547.

Skamarock, W. C., and Coauthors, 2008: A description of the Advanced Research WRF version 3. NCAR Tech. Note TN-475_STR, 113 pp.

Tao, W.-K., and Coauthors, 2003: Microphysics, radiation and surface processes in the Goddard Cumulus Ensemble (GCE) model. *Meteor. Atmos. Phys.,* **82,** 97–137.

Thu, T. V., and T. N. Krishnamurti, 1992: Vortex initialization for Typhoon track prediction. *Meteor. Atmos. Phys.,* **47,** 117–126.

Wang, Y., 2001: An explicit simulation of tropical cyclones with a triply nested movable mesh primitive equation model: TCM3. Part I: Model description and control experiment. *Mon. Wea. Rev.,* **129,** 1370–1394.

Wu, C.-C., K.-H. Chou, Y. Wang, and Y.-H. Kuo, 2006: Tropical cyclone initialization and prediction based on four-dimensional variational data assimilation. *J. Atmos. Sci.,* **63,** 2383–2395.

Xiao, Q., X. Zou, and B. Wang, 2000: Initialization and simulation of a landfalling hurricane using a variational bogus data assimilation scheme. *Mon. Wea. Rev.,* **128,** 2252–2269.

——, L. Chen, and X. Zhang, 2009: Evaluations of BDA scheme using the advanced research WRF (ARW) model. *J. Appl. Meteor. Climatol.,* **48,** 680–689.